

Tailoring of Physical and Chemical Properties of Macro- and Microhydrogels Based on Telechelic PVA

Gaio Paradossi,^{*,†} Francesca Cavalieri,[†] Ester Chiesi,[†] Valeria Ponassi,[†] and Vincenzo Martorana[#]

Department of Chemistry, University of Rome "Tor Vergata" and INFM, sezione Biofisica, UdR "Tor Vergata", Via della Ricerca Scientifica, Rome, Italy, and Biophysics Institute, CNR, section of Palermo, Via Ugo La Malfa, Palermo, Italy

Received July 26, 2002; Revised Manuscript Received September 17, 2002

Poly(vinyl alcohol), PVA, is amenable to several structural modifications because of the presence of the hydroxyl moiety in the backbone. The chemical versatility of this polymer can be used for the obtainment of new wall-to-wall pH-responsive PVA chemical hydrogels and for the preparation of air-filled microspheres, for example, microbubbles. Here, we report on the characterization of the physical and chemical properties of these novel networks that can be potentially used in different biomedical applications as controlled drug delivery and as ultrasonic contrast agent.

Introduction

Poly(vinyl alcohol), PVA, is a well-known synthetic polymeric material the biocompatibility of which justifies its inclusion in the class of biomacromolecules.¹ This characteristic comes jointly with a remarkable chemical versatility due to the presence of the hydroxylic moiety, which makes feasible a number of grafting modifications and of cross-linking reactions of the polymer backbone. In this paper, we report on some examples of modification/cross-linking of this biomacromolecule together with their characterization, bearing in mind the use of this polymer as biomaterial for potential applications in different field of biomedicine.

A modern biomaterial should have the capability to accomplish multitask functions as, for example, vitreoretinal surgery demands for new vitreous tamponade agents able to accomplish at the same time positional support and drug release therapy.² In this respect, PVA versatility is a good asset for complying with such demanding requirements.

Our laboratory is engaged in the development of PVA-based devices for different biomedical uses. In particular, focus is addressed to obtain new systems for drug delivery, tissutal substitutes, and, more recently, ultrasound contrast agents for diagnostic imaging. In this paper, we propose a few case examples on new PVA-based hydrogels exploiting the structural and chemical features of this polymer.

Some chemical hydrogels based on PVA are well-known in the literature.³ For their obtainment, use is made of toxic or at least not biocompatible molecules as cross-linking agents. On the other hand, physical hydrogels of PVA generated by a freeze–thaw cycles⁴ have in their opaqueness a major drawback for ophthalmological applications. High-

energy irradiation is another method for cross-linking PVA,⁵ but these networks containing aliphatic junction zones are not biodegradable. With these considerations in mind, we developed a synthetic route to chemical hydrogels of PVA in the absence of external cross-linkers but matching as much as possible the properties of clearness, biodegradability, and biocompatibility. This can be achieved by using as cross-linker a slightly modified PVA able to form with the hydroxylic moiety of PVA hydrolyzable chemical bonds. Moreover the cross-linking reaction is carried out without the addition of any external chemical agents, such as glutaraldehyde, able to decrease the biocompatibility of the resulting network.

Our approach in the synthesis of chemical hydrogels exploits the presence in the PVA chain of sporadic head-to-head sequences consisting of 1,2-glycolic units subjected to specific and quantitative splitting by periodate,⁶ a well-known reaction in carbohydrate chemistry.⁷ In this way, macromers of PVA, hereafter called *telechelic PVA*, bearing an aldehydic group at each end of the chain are obtained.

The amount of these sequences is small, about 1.5%, but detectable either by NMR or, as it was shown in a previous paper,⁸ by isothermal microcalorimetric titration. We used these reactive species for cross-linking intact PVA or telechelic PVA chain^{8–10} by means of an acetalization reaction between the aldehydic end groups of the cross-linker, that is, the telechelic PVA, and the hydroxylic moiety present in the PVA chains.

Gel-point determination and internal architecture of these matrixes were studied by different approaches, namely, compression modulus, swelling measurements, and dynamic light scattering.¹¹ Results showed that the average dimensions of the pore size of these systems range in the submicrometer distance scale, thus imparting to these hydrogels diffusive properties typical of nanostructured matrixes. The release properties of a polymeric matrix are related to this feature and to the diffusivity of water caged in the meshes of the

^{*} To whom correspondence should be addressed. E-mail address: paradossi@stc.uniroma2.it.

[†] University of Rome "Tor Vergata" and INFM.

[#] Biophysics Institute.

swollen network. To this aim, we undertook an incoherent quasi-elastic neutron scattering using as reference the glutaraldehyde-PVA swollen chemical hydrogel.¹²

This study showed a dynamic behavior of water in terms of its diffusion coefficient and relaxation times as a function of temperature. Within the frame of the unrestricted random jump model for treating quasi-elastic line broadening of the water peak, it appears clear that water entrapped in the gel network exists as supercooled water.¹³

In the context, we developed a method to obtain a charged PVA-based hydrogel starting from telechelic PVA to induce responsiveness to pH in PVA hydrogels, a property useful for designing PVA hydrogels as systems for drug delivery. In view of another potential use of PVA, we carried out the cross-linking of telechelic PVA at the air/solution interface, obtaining air-filled hollow microspheres, that is, microbubbles. These systems can be subjected to further development as "smart" micrometer-sized bubbles delivering selectively the bioactive agents into the cells by ultrasound activation. In this paper, we present two case examples showing that PVA can be innovatively exploited as polymeric material in biomedical fields such as controlled drug release and ultrasound imaging.¹⁴

Experimental Section

Materials. Poly(vinyl alcohol) was a Sigma product and used without further purification. The weight-average molecular weight measured by static light scattering is 67 000 g/mol. The degree of deacetylation determined by NMR was 0.98. Sodium metaperiodate, sodium chlorite, acetic acid, hydrochloric acid, and sodium hydroxide were Carlo Erba RPE products used without further purification. Deionized water (18 M Ω cm) was obtained with a USF Elga water deionizer.

Methods. Dynamic light scattering, DLS, was carried out with a Brookhaven BI2000 photometer equipped with a solid-state laser emitting at 532 nm. The vat containing Decalin as liquid for refractive index matching was thermostated at 25 °C. Homodyne-detected measurements at 90° were carried out using a pinhole aperture of 100 μ m with a 512 channel BI-9k correlator. Data analysis was carried out with CONTIN algorithm. Elastic light scattering measurements of the molecular weight of PVA were performed with the instrument on PVA aqueous solutions with concentrations ranging from 2 to 20 g/L and using a specific refractive index, dn/dc , of 0.164 mL/g.¹⁵ The reproducibility of these results were within $\pm 5\%$.

Light microscopy was performed on an Olympus CH-2 microscope.

Small-angle light scattering was carried out on an instrument based on a Fourier lens collecting on its focal plane the light scattered from the sample, according to the description available in the literature.¹⁶ A very small mirror, located on the lens focus, deviates the transmitted beam toward a photodiode. The focal plane is analyzed by a CCD camera. The images are acquired at different exposure times to allow for an expansion of the detectable intensity range. A single measurement gives the scattered light intensity over a q range going from 100 to 20 000 cm⁻¹. The instrument,

equipped with a He-Ne laser, has been calibrated using pinholes of diameter 25 and 59 μ m and tested using a dispersion of latex particles with nominal size of 3.6 and 9.4 μ m. Chemical stability of the microspheres was checked by repeating on the same sample the experiment after one month. Results were within 5%.

¹³C NMR spectra were recorded on a Bruker 400 MHz spectrometer using DMSO as reference. Potentiometric titrations were carried out on the protonated form of carboxylated telechelic PVA after ion exchange. A Radiometer potentiometer equipped with a semimicro combined glass electrode was used for the determination.

Scanning electron microscopy observations were performed on a Zeiss DSM 950 instrument operating at a voltage of 10 kV. Prior to examination, freeze-dried particles were deposited on aluminum stubs using a double-face adhesive tape and coated under vacuum with a thin layer of gold.

Synthesis of Telechelic PVA Containing Carboxylic Groups. The procedure was carried out according to the description of Hofreiter et al.¹⁷ A 30% (w/v) PVA aqueous solution is oxidized with NaIO₄, equimolar with the head-to-head sequences contained in the polymer. Acetic acid is added at room temperature to a concentration of 0.5 M followed by a 4-fold excess of NaClO₂ with respect to the aldehydic groups formed during the oxidation. The initial pH is 3.7, and the development in the solution of an intense red color is indicative of the reaction progress. After 4 h, the solution pH is 5.5. The polymer is precipitated by adding 2-propanol and then washed with a 9:1 2-propanol/water mixture.

Preparation of Hydrogels Containing Carboxylated Telechelic PVA. A 15% telechelic PVA aqueous solution is added with carboxylated telechelic PVA to a final polymer volume fraction of 20% (w/v). Addition of HCl started the cross-linking reaction. After 1 h, the reaction was stopped by neutralization. To minimize experimental errors, the gels were prepared using the same stock solution.

Conditioning of the gels at different pH was carried out as follows: Four cylindrical replicas were equilibrated with an aqueous solution containing a known amount of HCl or NaOH. The external solutions were renewed many times to replace the solvent contained in the gel phase and the final pH was measured.

Polymer volume fractions of swollen gels were measured by weighing out the gels after blotting for eliminating the superficial water excess.

Microbubbles Based on Telechelic PVA. A 2% (w/v) PVA aqueous solution is added with sodium metaperiodate in a equimolar ratio with the head-to-head sequences of the PVA chains. HCl as catalyst is added for the acetalization reaction. High-shear stirring is applied to the reaction mixture for 3 h with an Ultra Turrax stirrer at 8000 rpm. The cross-linking reaction is stopped by neutralizing the mixture, and the resulting suspension is dialyzed against water. Floating particles were separated from the precipitated material and collected in a water-containing jar.

Results and Discussion

Solution Characterization of Telechelic PVA. To obtain a PVA-based network with a swelling behavior displaying

the model suggested by Flory.²¹ In this treatment, the gel is considered an “elastic solution” rather than a viscous one. Its behavior is then dictated by three competing contributions to the solvent chemical potential, that is, a Flory–Huggins mixing term, $\Delta\mu_{1,\text{mixing}}$, a Donnan term caused by the localization of ionizable groups in the gel matrix and arising from difference in mobile ion concentration, $\Delta\mu_{1,\text{Donnan}}$, and an elastic term due to the presence of cross-links, $\Delta\mu_{1,\text{elast}}$.²¹ Assuming that the difference of chemical potential of the solvent, $\Delta\mu_1$, between the gel phase and the outside solvent can be written as the sum of the three terms mentioned above, the equilibrium condition for the swollen gel is determined according to eq 1:

$$\Delta\mu_1 = \Delta\mu_{1,\text{mix}} + \Delta\mu_{1,\text{elast}} + \Delta\mu_{1,\text{Donnan}} = 0 \quad (1)$$

The mixing term, $\Delta\mu_{1,\text{mix}}$, referring to the mixing of water and polymer can be expressed according to the Flory–Huggins theory²¹ as

$$\Delta\mu_{1,\text{mix}} = RT[\ln(1 - \phi_2) + \phi_2 + \chi_1\phi_2^2] \quad (2)$$

where ϕ_2 and χ_1 indicate the polymer network volume fraction at the maximum swelling and the polymer solvent interaction parameter, respectively.

The elastic term, $\Delta\mu_{1,\text{elast}}$ is the contribution relative to the elastic response of the network to the mixing and to the Donnan effect, corresponding to^{22,23}

$$\Delta\mu_{1,\text{elast}} = RTV_1\left(\frac{\nu_e}{V_0}\right)\phi_0\left[\left(\frac{\phi_2}{\phi_0}\right)^{1/3} - \frac{2}{3}\frac{\phi_2}{\phi_0}\right]L^{-1}(\lambda/\lambda_{\text{max}}) \quad (3)$$

where the ratio (ν_e/V_0) is the density of the chains effectively participating to the networking, ϕ_0 is the polymer volume fraction before the cross-linking process, λ is the extension ratio defined in terms of volume fraction as $\lambda = (\phi_0/\phi_2)^{1/3}$ and V_1 is the water molar volume. The presence of fixed charges on the network influences the elastic behavior of the gel phase as it is subjected to an inward osmotic flux of solvent causing the stretching of the network chains to a maximal extensibility, λ_{max} , with a consequent departure from the Gaussian behavior of the chains. To account for this effect, the original Flory–Rehner equation, assuming affine displacement of the cross-links and modified by Peppas et al.,²⁴ is modulated by the inverse Langevin function, L^{-1} , as predicted by the non-Gaussian chain statistics for an elongated chain.

In the case of networks containing fixed charges, the swelling process is governed by an additional term, the Donnan effect, due to the osmotic effect of the diffusible ions through the gel–solvent interface. In the investigated hydrogel, this effect is caused by the presence of fixed carboxylic charges introduced in the gel and determining an uneven distribution of ions diffusing at the interface between the gel phase and the solvent. This term will contribute to the overall change of solvent chemical potential with an osmotic term, $\Delta\mu_{1,\text{Donnan}} = -RTV_1\Delta c_{\text{tot}}$, competing together with mixing term against the elastic forces described in eq 3 and depending on the charge fraction and the ionic strength of the medium.

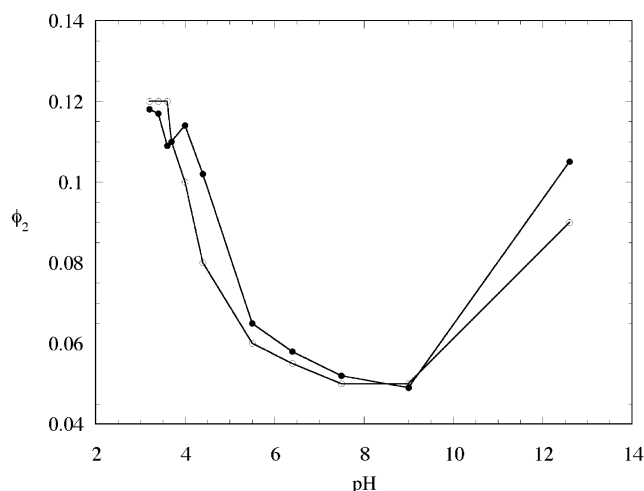


Figure 2. Swelling behavior of the PVA hydrogel containing carboxylated groups as a function of pH. Filled symbols indicate the experimental behavior; empty symbols are the theoretical behavior treated according to eq 1.

In our hydrogel at low pH, the Donnan effect is ineffective because the polymer carboxylic groups with an ionization constant pK_a of 4.00 are completely protonated. In this condition, the swelling behavior is dictated by the mixing and the elastic terms of eq 1 as for an uncharged network. When the pH is raised, the charge density of the gel phase increases while the ionic strength decreases. At the neutrality, the degree of ionization of the polymer is the unity whereas the external ionic strength is the lowest achievable. In these conditions, the largest excess of diffusible species in the gel with respect to the external phase and a considerable osmotic flux of solvent in the polymer phase are set and correspondingly the hydrogel reaches its highest degree of swelling. Increasing the pH to 12 causes a polymer charge screening reducing the unbalance of diffusible ion concentrations inside and outside the gel phase. These different states characterizing the dependence of the gel swelling behavior with pH are shown in Figure 2.

To treat the swelling in the investigated pH range, an evaluation of the $\Delta\mu_{1,\text{Donnan}}$ term is needed. The unbalance of mobile ions between the two phases, Δc , is defined as

$$\Delta c_{\text{tot}} = (c_+^{\text{in}} - c_+^{\text{out}}) + (c_-^{\text{in}} - c_-^{\text{out}}) \quad (4)$$

When the ionizable fixed charges *per* polymer chain are indicated by Z_p and the carboxylated PVA chain concentration in the gel phase as C_p with an ionization degree α , the difference in concentrations of the diffusible ions inside and outside the gel is

$$\Delta c_{\text{tot}} = Z_p C_p \alpha - \frac{4IZ_p C_p \alpha}{(6I + 4Z_p C_p \alpha)} \quad (5)$$

Z_p and C_p can be converted easily into the polymer volume fraction by means of

$$Z_p C_p = 2 \frac{\phi_2' \rho}{M_2} \quad (6)$$

with ρ , M_2 , and ϕ_2' indicating the density of the dry polymer, that is, 1.27 g cm⁻³, the molecular weight of the telechelic

chain, that is, 2000 g mol^{-1} , and the volume fraction relative to the carboxylated PVA component of the network, respectively.⁹

When different conditions of pH are explored, both α and the ionic strength, I , will vary according to the $\text{p}K_a$ of the carboxylic groups experimentally determined in the solution state. The dependence of the equilibrium polymer volume fraction on pH is obtained by summing up the three solvent chemical potential terms sorting the value of ϕ_2 at each pH that satisfies eq 1. In Figure 2, the calculated and experimental polymer volume fraction behaviors are reported.

Solving eq 1 with respect to ϕ_2 requires the estimation of the $\phi_{2\text{min}}$ parameter provided that χ and cross-linking density, ν_e/V_0 , are known. The χ value (0.54) at the same concentration of telechelic PVA was determined in a previous work.⁹

A cross-linking density, ν_e/V_0 , of $3.7 \times 10^{-4} \text{ mol cm}^{-3}$ was found as solution of the Flory–Rehner equation at low pH according to the Gaussian approach, which properly predicts the swelling behavior of nonionic network. L^{-1} can be accurately approximated by the Pade equation.²⁵ The limiting extension ratio λ_{max} can be expressed in terms of a reduced polymer volume fraction, ϕ_0 , relative to the minimum value achievable by the swollen gel at maximum chain elongation corresponding to $\phi_{2\text{min}}$:

$$\lambda_{\text{max}} = \left(\frac{\phi_0}{\phi_{2\text{min}}} \right)^{1/3} \quad (7)$$

This is an adjustable parameter because its evaluation cannot be obtained experimentally, because the maximum swelling obtainable in the gel may not correspond to the maximal chain extension, that is, when the chains of the network are completely stretched.

The limiting extension ratio λ_{max} is also given by²⁶

$$\lambda_{\text{max}} = \left(\frac{M_c}{M_s} \right)^{1/2} \quad (8)$$

where M_c and M_s are the molecular weight between two cross-links and the molecular weight of the statistical segment. The determination of λ_{max} allows for a value of M_c of about 3000 g/mol , which compares satisfactorily with the M_c obtainable from the chain density value evaluated at low pH, according to^{27,28}

$$M_c = \frac{\rho}{\left(\frac{\nu_e}{V_0} \right)} \quad (9)$$

The introduction of ionizable groups makes this novel PVA-based hydrogel responsive to the pH conditions of the external medium as the swelling increases a factor of 2 when passing from acidic or basic to neutral conditions.

Air-Filled Hollow Microspheres Based on Telechelic PVA. A potential application for telechelic PVA-based microgels can be envisaged as ultrasonic contrast agent in ecographic investigations. Enhanced backscattering modern contrast devices consist of air-filled hollow microspheres also called microbubbles or encapsulated gas bubbles.

According to the ultrasound backscattering process, the difference between the density of the medium and the core of the particles used as contrast agent is a major feature increasing the particle cross section with respect to the ultrasonic irradiation.^{29,30}

Biocompatibility is another unavoidable characteristic for such devices because they should be injected vascularly in the body. Recent available ultrasonic contrast agents are made by sonication of shell-forming materials such as human serum albumin or nonionic surfactant molecules. Obviously, the stability of the shell is crucial for the stability of the microbubbles both during storage and during in vivo application. In the context, we have developed a modification of the synthesis of the wall-to-wall telechelic PVA-based network by carrying out the cross-linking process at the air/solution interface with the assistance of high-shear stirring. The resulting dispersion is mainly constituted by a precipitated material and a floating material. Light microscope observations, Figure 3, showed that the floating fraction consisted of microspheres of the diameter of about $4 \mu\text{m}$ while the precipitated part of the dispersion was made mainly of aborted particles or polymeric debris.

AFM micrographs (not shown) and SEM image confirmed the former observations. Figure 4 shows that the freeze-drying process carried out on a hollow microsphere sample has collapsed the system.

A possible formation process of the floating microspheres is briefly outlined. Telechelic building blocks move onto the newly created gas–liquid interface with the hydrophobic portions of the macromolecules facing toward the gas phase and the hydrophilic moiety facing toward the aqueous medium. Organization of telechelic poly(vinyl alcohol) into micellar assemblies is stabilized by covalent intramolecular cross-linking in which a thick shell layer imparts high-shear resistance to the particles. Free aldehydic groups evidenced on the surface by FTIR specular reflectance (not shown) indicate a partial acetalization and allow for covalent coupling of targeting ligands to the preformed bubbles or for modification of surface properties of PVA microbubbles.

The microparticles were analyzed by dynamic light scattering, DLS, to get an estimate of their average hydrodynamic dimensions. The tendency to flotation complicated the DLS observations because it was introducing a preferential directionality in the diffusion process of the particles. In any case, Brownian diffusion was completely decoupled from floating direction, developing at much shorter time scale than the vertical migration of the particles. Only the shorter correlation time was therefore analyzed in the correlation function. The measurements yielded a hydrodynamic parameter in agreement with light microscopy.

The tendency to float in water is an evidence that the particles were hollow and filled with air. The possibility that the particles were floating in water for a surface tension effect was ruled out by the observation that the addition to the system of the surfactant Tween 80 did not perturb the particle floating.

A further characterization of these microparticles was carried out by studying the static light scattering at very low angles, SALS. The analysis of the scattering data is depend-

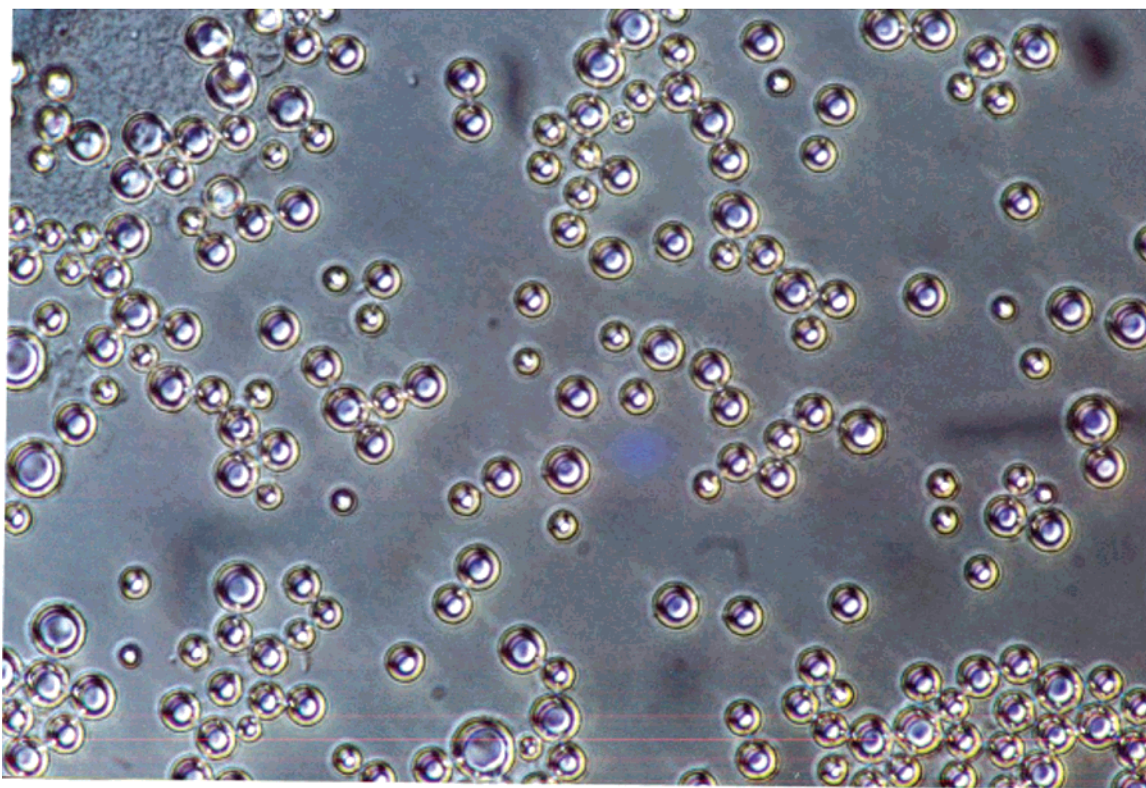


Figure 3. Light micrograph of a dispersion of microbubbles ($\times 1000$).

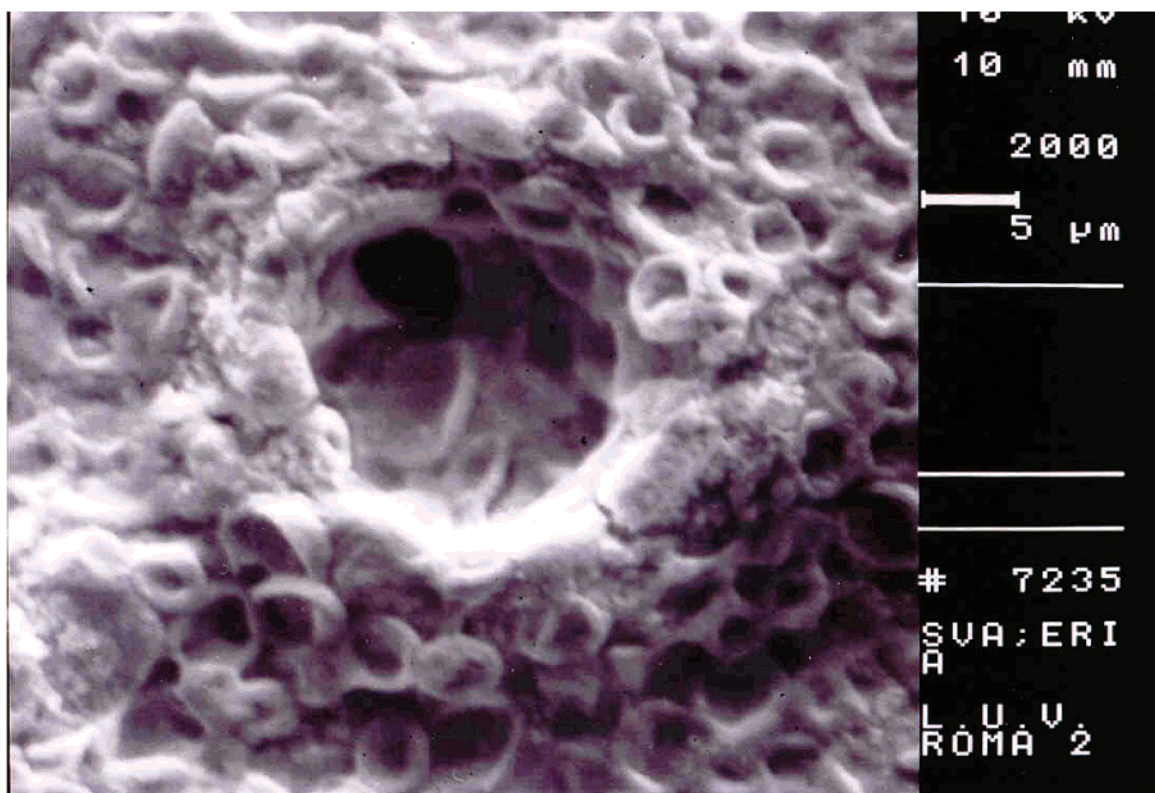


Figure 4. SEM micrograph of a freeze-dried sample of collapsed hollow microspheres.

ent on the dimensions of the observed particles. We have chosen to treat in our analysis the microparticles as Rayleigh scatterers, although the diameter size of this system places the interpretation of the observed q dependence of the

scattered intensity somewhat at the border between the Rayleigh and Mie scattering behavior. The experimental shape factor of the particle was analyzed in terms of two models: (i) a spherical model (eq 10a) with a Gaussian size

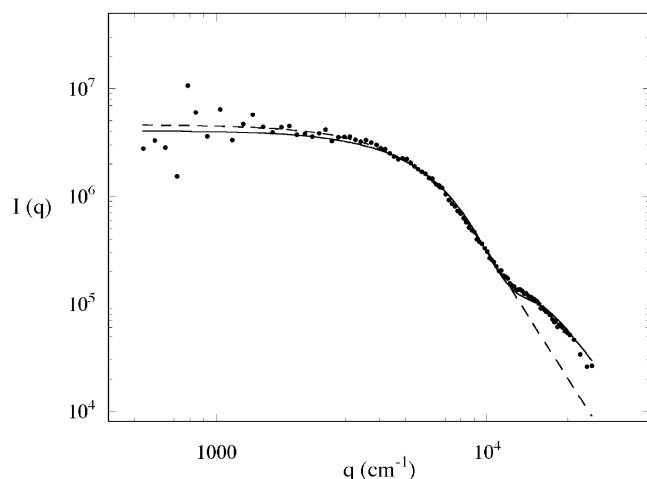


Figure 5. Small angle light scattering study of a dispersion of microbubbles (filled circles). Dashed line indicates the fit with the model relative to the hard microsphere; continuous line is the fit relative to the hollow microsphere model.

distribution and (ii) a hollow sphere model (eq 10b) described in terms of internal and external radii with a Gaussian size distribution.³¹

$$P(q) = \left\{ \frac{3}{(qR_s)^3} [\sin(qR_s) - (qR_s) \cos(qR_s)] \right\}^2 \quad (10a)$$

$$P(q) = \left\{ \frac{3}{(qR_s)^3 \left(1 - \frac{R_i}{R_s}\right)} [\sin(qR_s) - \sin(qR_i) - (qR_s) \cos(qR_s) + (qR_i) \cos(qR_i)] \right\}^2 \quad (10b)$$

The structure factor for a hollow sphere has as distinctive feature, the presence of a more pronounced secondary maxima in the high q region with respect to the behavior of the $P(q)$ of a hard sphere. This difference is smeared out by polydispersity,³² that is, in the case of highly polydispersed hollow spheres the scattering function can closely resemble that of a hard sphere. As it is shown in Figure 5, the two models could fit satisfactorily both the low and intermediate q region of the shape function, whereas in the high q region only, the second model was able to fit the experimental shape function, confirming that the floating fraction collected was constituted by hollow microspheres with limited polydispersity. It should be pointed out that these hollow microsphere samples were obtained without any preliminary fractionation process.

Interpretation of the experimental findings in terms of a bimodal size distribution can be ruled out also by considering that the DLS correlation curves have evidenced a Gaussian distribution of the hydrodynamic radii. The fit based on the hollow sphere model allowed also an estimate of the thickness of the sphere resulting in about 1.1 μm . Further investigation concerning density measurements of the particles will help in the complete characterization of this system, together with biocompatibility tests. In Table 1, the relevant characteristic parameters of the hollow microspheres collected by means of different methods are reported.

Table 1. Characteristic Dimensions of the Microparticles Obtained by Different Methods

	external radius (μm)	internal radius (μm)
AFM ^a (wet sample)	3.2 \pm 0.1	
SEM (dry sample)	2.7 \pm 0.1	
light microscopy	\approx 3.0	
DLS	2.7 ^b \pm 0.1	
SALS	2.7 \pm 0.2	1.6 \pm 0.2

^a Not shown in this work. ^b Hydrodynamic radius, R_h .

Considering that the radius of gyration, R_g , and the external radius, R , of a hard sphere are related by the relationship $R = (5/3)^{0.5} R_g$ and the R_g of an infinitely thin hollow sphere is identical to its external radius, we conclude that for our empty spheres with a finite thickness of the shell the external radius is about 1.1 times the corresponding radius of gyration. It is worth noting that the ratio ρ defined as R_g/R_h , where R_h is the hydrodynamic radius evaluated by DLS method, is equal to 0.91 for our hollow spheres. This value falls in the range predicted by the theory because a value of 1 and of 0.775 for ρ of the infinitely thin hollow sphere and of the hard sphere, respectively, has been found.³² This check can be regarded as a validation of the treatment of our data within the frame of Rayleigh scattering theory.

Concluding Remarks

Taking advantage of the chemical versatility of PVA, we investigated the structure properties of a carboxylated telechelic charged PVA in this study. This macromer was used for the obtainment of a pH-responsive PVA macrohydrogel. The behavior of this network was studied in terms of the Flory–Rehner swelling theory taking into account the presence of ionizable charges contained in the gel phase. The responsiveness to external stimuli such as pH and ionic strength allows us to envisage a potential use of this system as matrix for controlled drug delivery.

Carrying out the cross-linking reaction of telechelic PVA at the water/solution interface, we obtained narrowly polydispersed air-filled microspheres potentially suitable as vascularly injectable ultrasonic contrast agent. These two case examples, far to be fully developed, are representative of the versatility of PVA as starting polymer material for the formulation of new systems for potential biomedical applications. Functionalization for multitask purposes is the next step for the engineering of these systems. The unreacted aldehydic groups or the PVA hydroxylic moiety or both can be used to obtain hollow microspheres with receptor-coated surface for tissues/organs targeting.

References and Notes

- (1) Pritchard, J. G. *Polyvinyl Alcohol. Basic properties and applications*; Gordon and Breach: London, 1970.
- (2) Colthurst, M. J.; Williams, R. L.; Hiscott, P. S.; Grierson, I. *Biomaterials* **2000**, *21*, 649–665.
- (3) Mackenna, G.; Horkay F. *Polymer* **1994**, *35*, 5737.
- (4) Peppas, N. A.; Scott, J. E. *J. Controlled Release* **1992**, *18*, 95–100.
- (5) Ulanski, P.; Janik, I.; Rosiak, J. M. *Radiat. Phys. Chem.* **1998**, *52*, 289–294.
- (6) Flory, P. J.; Leutner, F. S. *J. Polym. Sci.* **1948**, *3*, 880–887.
- (7) Painter, T.; Larsen, B. *Acta Chem. Scand.* **1970**, *24*, 2724–2736.
- (8) Paradossi, G.; Lisi, R.; Paci, M.; Crescenzi, V. *J. Polym. Sci., Polym. Chem. Ed.* **1996**, *34*, 3417–3425.

- (9) Paradossi, G.; Cavalieri, F.; Capitani, D.; Crescenzi, V. *J. Polym. Sci., Polym. Phys. Ed.* **1999**, *37*, 1225–1233.
- (10) Paradossi, G.; Cavalieri, F.; Crescenzi, V. *Recent Res. Dev. Polym. Sci.* **1999**, *3*, 1–12.
- (11) Barretta, P.; Bordini, F.; Rinaldi, C.; Paradossi, G. *J. Phys. Chem. B* **2000**, *104*, 11019–11026.
- (12) Paradossi, G.; Di Bari, M. T.; Telling, M. T. F.; Turtu', A.; Cavalieri, F. *Physica B* **2001**, *301*, 150–156.
- (13) Teixeira, T.; Bellisent-Funel, M. C.; Chen, S. H.; Dianoux, A. J. *Phys. Rev. A* **1985**, *31*, 1913–1917.
- (14) Unger, E. C.; Matsunaga, T. O.; McCreery, T.; Schumann, P.; Sweitzer, R.; Quigley, R. *Eur. J. Radiol.* **2002**, *42*, 160–168.
- (15) Brandrup, J.; Immergut, E. H.; Grulke, E. A. *Polymer Handbook*; Wiley-Interscience: New York, 1999.
- (16) Ferri, F. *Rev. Sci. Instrum.* **1997**, *68*, 2265–2274.
- (17) Hofreiter, B. T.; Wolff, I. A.; Mehlretter, C. L. *J. Am. Chem. Soc.* **1957**, *79*, 6457–6464.
- (18) Crescenzi, V.; Gamini, A.; Paradossi, G.; Torri, G. *Carbohydr. Polym.* **1983**, *3*, 273–286.
- (19) Ando, I.; Kobayashi, M.; Kanekiyo, M.; Kuroki, S.; Ando, S.; Matsukawa, S.; Kurosu, H.; Yasunaga, H.; Amiya, S. NMR Spectroscopy in Polymer Science. In *Experimental Methods in Polymer Science*; Tanaka, T., Ed.; Academic Press: San Diego, CA, 2000.
- (20) Kobayashi, M.; Ando, I.; Ishii, T.; Amiya, S. *Macromolecules* **1995**, *28*, 6677–6679.
- (21) Flory, P. J. *Principles of Polymer Chemistry*; Cornell University Press: Ithaca, NY, 1953; Chapter XIII.
- (22) Flory, P. J.; Rehner, J., Jr. *J. Chem. Phys.* **1943**, *11*, 521–530.
- (23) Opperman, W. In *Polyelectrolyte Gels, Properties, Preparation and Applications*; Harland, R. S., Proud'homme, R. K., Eds.; American Chemical Society: Washington, DC, 1992.
- (24) Treloar, L. R. G. *The Physics of Rubber Elasticity*; Clarendon Press: Oxford, U.K., 1975.
- (25) Peppas, N. A.; Merrill, E. W. *J. Polym. Sci., Polym. Chem. Ed.* **1976**, *14*, 459–464.
- (26) Haward, R. N. *Polymer* **1999**, *40*, 5821–5832.
- (27) Meissner, B. *Polymer* **2000**, *41*, 7827–7841.
- (28) Queslel, J. P.; Mark, J. E. *Polym. Bull.* **1983**, *10*, 119–125.
- (29) Ophir, J.; Parker, K. J. *Ultrasound Med. Biol.* **1989**, *15*, 319–333.
- (30) Correias, J. M.; Bridal, L.; Lesavre, A.; Mejean, A.; Claudon, M.; Helenon, O. *Eur. Radiol.* **2001**, *11*, 1316–1328.
- (31) Schmitz, K. S. *An Introduction to Dynamic Light Scattering by Macromolecules*; Academic Press: San Diego, CA, 1990.
- (32) Stauch, O.; Schubert, R.; Savin, G.; Burchard, W. *Biomacromolecules* **2002**, *3*, 565–578.

BM0256247